



NRC Publications Archive Archives des publications du CNRC

Proposed Traceable Structural Resolution Protocols for 3D Imaging Systems

MacKinnon, David; Beraldin, J.-Angelo; Cournoyer, Luc; Carrier, Benjamin;
Blais, François

This publication could be one of several versions: author's original, accepted manuscript or the publisher's version. /
La version de cette publication peut être l'une des suivantes : la version prépublication de l'auteur, la version
acceptée du manuscrit ou la version de l'éditeur.

Publisher's version / Version de l'éditeur:

Proceedings of the Videometrics, Range Imaging and Applications X, 2009, 2009-08-03

NRC Publications Record / Notice d'Archives des publications de CNRC:

<https://nrc-publications.canada.ca/eng/view/object/?id=bca57969-ed30-42a7-adc5-a15cf9207f13>
<https://publications-cnrc.canada.ca/fra/voir/objet/?id=bca57969-ed30-42a7-adc5-a15cf9207f13>

Access and use of this website and the material on it are subject to the Terms and Conditions set forth at

<https://nrc-publications.canada.ca/eng/copyright>

READ THESE TERMS AND CONDITIONS CAREFULLY BEFORE USING THIS WEBSITE.

L'accès à ce site Web et l'utilisation de son contenu sont assujettis aux conditions présentées dans le site

<https://publications-cnrc.canada.ca/fra/droits>

LISEZ CES CONDITIONS ATTENTIVEMENT AVANT D'UTILISER CE SITE WEB.

Questions? Contact the NRC Publications Archive team at

PublicationsArchive-ArchivesPublications@nrc-cnrc.gc.ca. If you wish to email the authors directly, please see the first page of the publication for their contact information.

Vous avez des questions? Nous pouvons vous aider. Pour communiquer directement avec un auteur, consultez la première page de la revue dans laquelle son article a été publié afin de trouver ses coordonnées. Si vous n'arrivez pas à les repérer, communiquez avec nous à PublicationsArchive-ArchivesPublications@nrc-cnrc.gc.ca.



Proposed Traceable Structural Resolution Protocols for 3D Imaging Systems

David MacKinnon,* J.-Angelo Beraldin, Luc Cournoyer, Benjamin Carrier, and François Blais

National Research Council of Canada, Ottawa, Ontario, Canada

ABSTRACT

A protocol for determining structural resolution using a potentially-traceable reference material is proposed. Where possible, terminology was selected to conform to those published in ISO JCGM 200:2008 (VIM) and ASTM E 2544-08 documents. The concepts of resolvability and edge width are introduced to more completely describe the ability of an optical non-contact 3D imaging system to resolve small features. A distinction is made between 3D range cameras, that obtain spatial data from the total field of view at once, and 3D range scanners, that accumulate spatial data for the total field of view over time. The protocol is presented through the evaluation of a 3D laser line range scanner.

Keywords: resolution, quality metrics, laser range imaging, laser range scanner, 3D metrology

1. INTRODUCTION

The three most important metrics for any **measuring system**¹ are **measurement resolution**,¹ **measurement accuracy**,¹⁻³ and **measurement precision**,^{1,2} which have been defined by the Joint Committee for Guides in Metrology (JCGM) for a broad range of measurement systems. Accuracy is quantified by **measurement error**^{1,3} and precision by the **standard measurement uncertainty**.¹⁻³ Quantifying resolution is particularly challenging for **3D imaging systems**² and there is currently no commonly-accepted definition of spatial resolution⁴ or even standardized protocols for evaluating the spatial resolution of 3D imaging systems.^{5,6} Resolution, accuracy and precision are interrelated so quantifying spatial resolution requires taking all three parameters into account. In this paper, resolution is defined as an extension to existing ISO JCGM 200:2008 (VIM)¹ and ASTM E 2544-08 (ST3DIS)² vocabularies, and is quantified with respect to a potentially-traceable **certified reference material**¹ using a proposed **reference measurement procedure**.¹ Methods for quantifying precision are only addressed peripherally in this paper.

2. BACKGROUND

3D imaging systems can be divided into 3D range scanners and 3D range cameras. A **3D range camera** can be defined as a **measuring instrument**¹ in which spatial **measurement results**^{1,3} are acquired simultaneously for the total field of view. 3D range cameras generate an output signal in which the measurement result is, minimally, a set of simultaneously-generated vectors containing spatial information in the form of a distance **measured quantity value**¹ and two coordinate measured quantity values. A **3D range scanner** can be defined as a **measuring system**¹ in which spatial measurements are obtained sequentially from within the total field of view. The term “system” is used rather than device because the final spatial measurement result is generated from two or three separate measuring devices: one that obtains a distance measured quantity value and possibly a measured quantity value result along one coordinate axis, and one or two devices that each generate measured quantity values from the remaining coordinate axis or axes. The results presented in this paper apply only to 3D range scanners.

Parallax is an issue that particularly affects short-range (<1 metre) 3D imaging systems. Often the optical **sensor**¹ is separated from the optical emitter by a distance, referred to as the baseline, that is large compared to the distance between the 3D imaging system and the surface being imaged. The length of the baseline is used to compute the range measurement result in triangulation-based systems. Few medium-range (1 to 10 metres) and long-range (>10 metres) systems use triangulation; in time-of-flight-based systems the emitter and detector paths are either collinear or have negligible parallax. Only short-range 3D range scanners were used in this study so that parallax would be a significant **influence quantity**.^{1,3}

*Corresponding author: david.mackinnon@nrc-cnrc.gc.ca

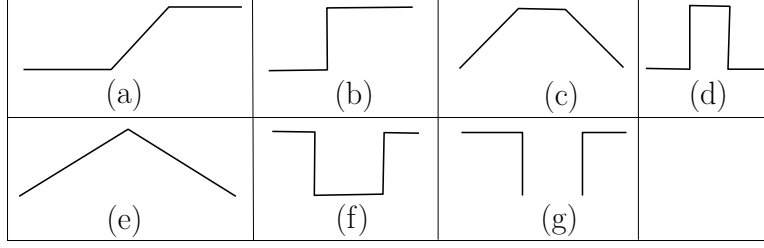


Figure 1. Types of edges. (a) Ramp (b) Step (c) Ridge (d) Post (e) Roof (f) Pit (g) Gap

2.1 Resolution

Representing the resolution of a 3D imaging system is a complex problem. The annex to the VDI/VDE 2617 Part 6.2⁷ divides resolution for 3D imaging systems into **spatial resolution**⁷ and **structural resolution**⁷. Spatial resolution is defined as characterizing the smallest measurable displacement along each of the 3 axes of measurement and is similar to the **discrimination threshold**.¹ Structural resolution defined as the size of the smallest structure measurable within some defined set of **maximum permissible errors**;^{1,2} however, there is little agreement on the type of structure, or structures, that should be measured.

Edges are the most common types of structures and can be classified as **step-edge**, **ramp-edge**, **ridge-edge**, and **roof-edge** [8, pp.71-72], as illustrated in Figure 1. Step-edges are ramp-edges in which the transition between surfaces appears to the 3D imaging system as instantaneous, while roof-edges are ridge-edges in which the top of the ridge cannot be resolved by the 3D imaging system. We further define a **post-edge** as a ridge-edge in which the transition between surfaces appears to the 3D imaging system as instantaneous. Related to the edge is the **pit**, in which a surface region is bounded by surfaces that are closer to the 3D imaging system. We define a **gap** as a pit in which the surface farthest from the 3D imaging system is beyond the resolvable range of the system. The structural resolution of a 3D imaging system can be characterized by how well it handles each of these structures.

The VDI/VDE 2617 Part 6.2⁷ proposes using a right-angled edge structure, such as a step-edge as illustrated in Figure 1(b) or post-edge as illustrated in Figure 1(d), and analyzing the edge profile to obtain a measure of the structural resolution of the system. Specifically the structural resolution is approximated by the spatial frequency at which the magnitude of the transfer function drops by 3-dB. In practice, factors like parallax result in partial occlusion of either the optical sensor or optical emitter make it difficult to obtain a complete spatial step-response along the baseline axis of the 3D imaging system. This approach also ignores edge structures like ramp-edges and roof-edges which behave differently than step-edges and step-like edges. We propose using a simplified analysis of both step-edge and roof-edge structures to characterize two aspects of the structural resolution of a 3D imaging system.

3. PROPOSED METHODOLOGY

The proposed methodology consists of three stages: fitting the CAD model to the measured data, obtaining the average roof-edge spatial response cut-off-value (resolvability structural resolution metric $f_{resolve}$) and the **repeatability**^{1,3} of the metric, and obtaining the step-edge spatial response cut-off value (edge width structural resolution metric f_{edge}) and the repeatability of the metric. For purposes of discussion, all measured quantity values are assumed to be in the Cartesian coordinate system with the x-axis representing the primary scan axis, the y-axis representing the secondary scan axis, and the z-axis representing the depth axis. For the line scanner used in this experiment, the primary axis is the axis formed by the line and the secondary axis is the direction of motion of the translation stage as shown in Figure 2.

Ideally, all structural resolution metrics should be obtained using a **reference material**¹ (RM) for which the associated CAD model has a precision and accuracy at least one order of magnitude smaller than the expected



Figure 2. SG-series laser line scanner mounted on a translation stage

limits of the 3D imaging system under test. The CAD model should include the degree of rounding of all edges based on a profilometric analysis of each edge. An analysis should be performed to verify the degree of flatness of all surfaces.

All of the stages are performed for repeated measurements of the same surface under the same test conditions (**repeatability conditions**¹⁾) to obtain the **average**³ of $f_{resolve}$ and f_{edge} , and the repeatability (**experimental standard deviation**³), $s_{resolve}$ and s_{edge} respectively, of each structural resolution metric. At least 10 repetitions are performed to obtain results with an α -risk and β -risk of $p_\alpha < 0.05$ and $p_\beta > 0.80$ respectively, where p_α and p_β are the **confidence levels**⁹ in being able to minimize Type I* and Type II† errors respectively, and a statistical resolution[‡] equal to the sample standard deviation [10, pp.395-398]. Additional repetitions can be performed to increase the statistical resolution to the desired level, provided the repeatability conditions are maintained.

3.1 CAD Model Fitting

The measured depth values must be preserved in order to calculate each of the structural resolution metrics so the CAD model must be fit to the measured data. A precise and accurate fit is required because the CAD model is used to represent the location of the edges used in subsequent stages. The fitting procedure is as follows:

1. in the measured data, the spherical targets are manually located and tagged;
2. spherical targets in the CAD model with the same tag are used to perform an initial fit of the CAD model to the data; and
3. measured data within the inner portion of each roof surface are combined with the corresponded spherical targets in the measured and CAD data to perform a final fit.

The fitting procedure requires the spherical targets in the CAD model to have been tagged in a pre-defined sequence so that the spherical targets can be correctly corresponded with the spherical targets located and tagged in the measured data. Planar fitting is performed for the final fit to improve the correspondence between the CAD and measured data. Only the inner portion of each planar surface is used to ensure no measured value has been affected by an edge.

3.2 Resolvability Analysis

The roof-edge spatial response is the measured roof width per unit CAD roof width versus the CAD roof width, and is based on the method first proposed by Goesele et al.¹¹ to measure the structural resolution of a 3D range scanner without including the effect of spatial or intensity discontinuities. The roof-edge procedure is as follows:

1. measured data is selected that corresponds to the peak of the roof-edge but not including any other edges;
2. the measured data is collapsed along the axis formed by the peak of the roof-edge in the CAD model to form a super-resolution line;
3. the super-resolution line of measured data is binned along the depth axis into subsamples separated by a depth interval (sub-sampling density) Y_S for both roof surfaces;
4. the within-bin distance between each of the roof surfaces (roof width) is obtained for the measured and CAD data;
5. the decibel ratio of the within-bin measured roof width to within-bin CAD roof width (gain) is plotted against the base-10 log of the inverse of the CAD roof width (spatial frequency); and
6. the spatial response cut-off value $f_{resolve}$ is obtained as the spatial frequency at which the gain falls by 3 dB, as illustrated in Figure 3(a).

*False positive: the probability of incorrectly rejecting a true null hypothesis

†False negative: the probability of incorrectly accepting a false null hypothesis

‡The statistical resolution is the minimum inter-group separation that would result in the groups being considered significantly different with a confidence level of $1 - \alpha$ if the predicted and observed variances remain the same.

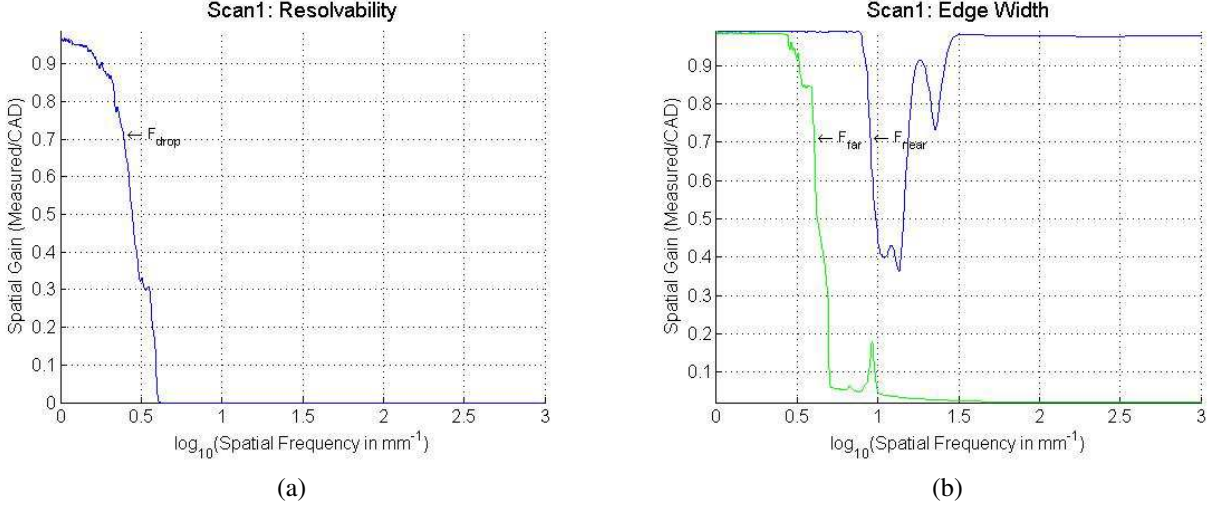


Figure 3. (a) Resolvability and (b) edge width of an SG-102 laser line scanner at 0.10 millimeters inter-line separation.

The method presented here differs from the original proposed method in several key aspects. First, instead of using a derivative filter to locate the peak in each of the scan lines, the method proposed here uses the location of the peak edge obtained from the CAD model. Second, rather than calculating the transfer function of the system using a discrete Fourier transform, the response gain is obtained from the decibel ratio of the measured to CAD roof width and the frequency component is the inverse of the CAD roof width. This approach is computationally simple and results in a $f_{resolve}$ value that is easy to interpret as the inverse of the peak width at which the ability to reproduce the roof-edge falls by 3 dB.

3.3 Edge Width Analysis

The step-edge spatial response is the absolute deviation between the measured and CAD depth values versus the width of the edge region, and is based on the ISO 12233¹² slanted-edge method for determining the lateral resolution of photographic systems. The step-edge procedure is as follows:

1. measured data is selected that corresponds to the peak of the step-edge but not including any other edges;
2. the measured data is collapsed along the axis formed by the peak of the step-edge in the CAD model to form a super-resolution line;
3. the super-resolution line of measured data is binned along the lateral axis into subsamples separated by a lateral interval (sub-sampling density) Y_S for both step surfaces;
4. the absolute within-bin distance between the measured and CAD data (depth discrepancy) is obtained for each of the roof surfaces;
5. the decibel ratio of the absolute within-bin discrepancy to within-bin depth maximum separation between step surfaces (gain) is plotted against the base-10 log of the inverse of the lateral distance to the edge in the CAD model (within-surface spatial frequency) for both step surfaces;
6. the within-surface spatial response cut-off values f_{near} and f_{far} are obtained for the near and far step surfaces respectively as the spatial frequency at which the gain falls by 3 dB, as illustrated in Figure 3(b); and
7. the combined spatial response cut-off value f_{edge} is the inverse of the lateral distance between the 3 dB points of each step surface.

The method presented here differs from the ISO 12233 method in several key aspects. First, instead of using a derivative filter to locate the peak in each of the scan lines, the method proposed here uses the location of the peak edge obtained from the CAD model. Second, rather than calculating the transfer function of the system using a discrete Fourier transform, the

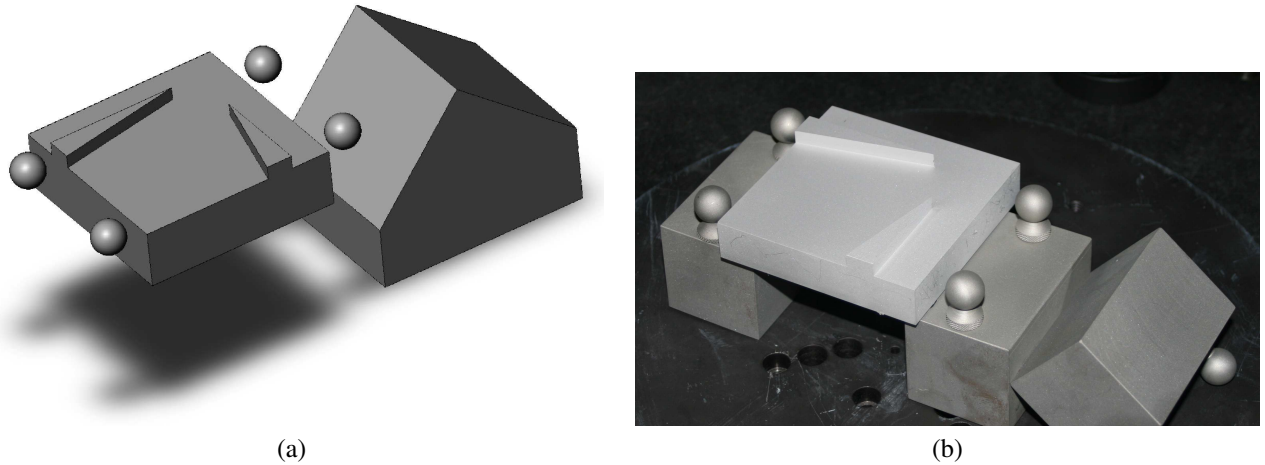


Figure 4. (a) CAD model of material measure designed by NRC. (b) Photograph of material measure.

response gain is obtained from the ratio of the range discrepancy to the CAD surface-to-surface separation. The f_{edge} metric represents the width of the edge region (edge width) arising from the presence of a discontinuity, while the within-surface spatial response values represent the size of the edge region on the near-depth and far-depth surfaces. This approach is computationally simple and results in an f_{edge} value that is easy to interpret as the inverse of the width of the region around a step-edge within which the ability to reproduce the step-edge falls by 3 dB. This approach is also robust to occlusion, which can make it difficult to obtain the Fourier transform of the edge profile unless the Fourier transform has been adapted for data with unequal sample sizes, or missing data within each bin has been approximated using some form of interpolation.

4. EXPERIMENTAL RESULTS

An RM illustrated in Figure 4, was created so that data for both test methods could be collected in a single scan. The RM consists of four tooling spheres, a dual-wedge surface, and a rectangular block oriented to present one edge to the 3D laser range scanner. All surfaces were vapour-blasted to ensure uniform reflectivity. At the time of this writing, a reference material conforming to the standards discussed in Section 3 was still under construction so was not available for testing. All results were, therefore, obtained using a rough model of the reference material for which edge profilometry and an analysis of the flatness of all planar surfaces was not completed.

A Shapegrabber® SG-102 short-range 3D laser range scanner* was used to collect 10 range images at 0.05 and 0.10 mm inter-line spacing with the x-axis corresponding to the laser line and the y-axis corresponding to the scanner translation. The SG-102 has a reported lateral resolution of between $\Delta x_{near} = 0.07$ and $\Delta x_{far} = 0.14$ millimeters along the x-axis (laser line axis) and as little as $\Delta y = 0.02$ millimeters along the y-axis (translation axis).¹³ Two inter-line separations were used during testing to assess the **reproducibility**^{1,3} of the structural resolution metrics. The CAD model was generated using Solidworks[†] based on data collected using a Faro Gage Plus[‡]. The Faro® Gage Plus has a reported lateral measurement uncertainty of $s_{lat} = 0.005$ millimeters¹⁴ so group means must be separated by at least 0.01 millimeters for any significant differences to have practical significance. Each range image was imported into Polyworks[§] where the spheres were selected and modeled, as illustrated in Figure 5(a). The range image was then exported to Matlab^{||} for initial fitting based on correspondence between tagged spheres in measured and CAD data, followed by final fitting based using a 5×5 millimeter section at the center of each roof surface, as illustrated in Figure 5(b). Resolvability and edge width structural resolution metrics were then generated for each range image using Matlab. All test results were then exported to Mathematica^{||} where the mean and standard deviation of each set of 10 range images was generated, and all statistical tests were performed.

*<http://www.shapegrabber.com/sol-products-3d-scan-heads-sg2.shtml>

†<http://www.solidworks.com/>

‡<http://www.faro.com/content.aspx?ct=uk&content=pro&item=4&subitem=9>

§<http://www.innovmetric.com/>

||<http://www.mathworks.com/>

||<http://www.wolfram.com/products/mathematica/index.html>

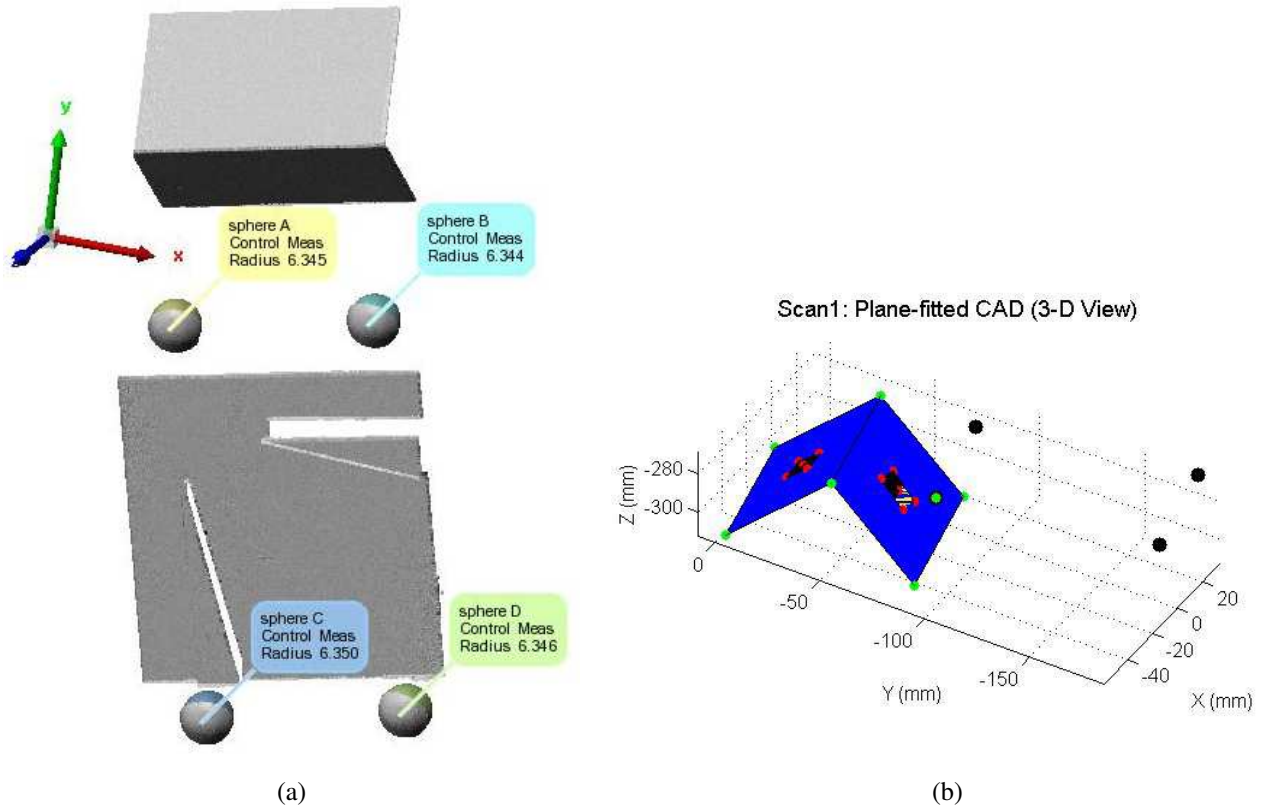


Figure 5. (a) Example of a range image in Polyworks after sphere selection and labeling. (b) The black square on each surface represents the planar regions used in final fitting.

The resolvability and edge width structural resolution metrics were used to examine the effect of changing inter-line separation on the structural resolution of the SG-102 laser line scanner. Table 1 shows the results of varying the inter-line separation on each the resolvability (mm^{-1}) and edge width (mm^{-1}) structural resolution metrics with a sub-sampling density of $Y_S = 1/1000 \text{ mm}$. Comparisons of means was performed using a t-test⁹ and comparisons of variances were performed using the F-ratio test. The variable N refers to the number of samples in each group. Groups within each row are significantly different if the significance level is less than 0.05 and have been bolded for ease of identification.

As can be seen in Table 1, there was no significant difference in resolvability and edge width variances so the t-tests could be performed under the assumption of equal variances. The resolvability of the SG-102 using a 0.05 millimeter inter-sample distance ($f_{\text{resolve}} = 2.41 \text{ mm}^{-1}$ or a peak width of $1/f_{\text{resolve}} = 0.415 \text{ mm}$) was significantly lower than when using a 0.10 millimeter inter-sample distance ($f_{\text{resolve}} = 2.43 \text{ mm}^{-1}$ or a peak width of $1/f_{\text{resolve}} = 0.412 \text{ mm}$); however, this effect is smaller than the 0.010 millimeter lower imposed by the measurement uncertainty of the Faro Gage Plus so has no practical significance. The edge width of the SG-102 using a 0.05 millimeter inter-sample distance ($f_{\text{edge}} = 2.88 \text{ mm}^{-1}$ or a edge region width of $1/f_{\text{edge}} = 0.347 \text{ mm}$) was significantly higher than when using a 0.10 millimeter inter-sample distance ($f_{\text{edge}} = 2.80 \text{ mm}^{-1}$ or a edge region width of $1/f_{\text{edge}} = 0.357 \text{ mm}$). The inter-group difference is equal to the Faro Gage Plus measurement uncertainty limit of 0.01 millimeters so this effect has marginal practical significance. In general, the edge width metric was able to detect that reducing the inter-line distance decreases (improves) the structural resolution of the SG-102. The $1/f_{\text{resolve}}$ and $1/f_{\text{edge}}$ values are considerably larger than the Δx_{far} , Δx_{near} , and Δy values reported for the SG-102, but are not considerably different than each other.

The reproducibility of the resolvability and edge width structural resolution metrics were examined by varying both the inter-line separation and the sub-sampling density Y_S . A two-way Analysis of Variance (ANOVA) test was used to test the assumption that the means of each group are equal. The significance level of the inter-line separation, sub-sampling density, and the interaction between inter-line separation and sub-sampling density are shown in Table 2. As was the case

Table 1. Effect of inter-line separation on the resolvability (mm^{-1}) and edge width (mm^{-1}) of an SG-102 laser line scanner. Results are presented as mean \pm standard deviation. The Means comparison column shows the significance level of the t-test. The Variance comparison column shows the significance level of the F-ratio test. The variable N refers to the number of samples in each group. Groups within each row are significantly different if the significance level is less than 0.05. Significance levels less than 0.001 are represented as ≈ 0 and those larger than 0.999 are represented as ≈ 1 . Sub-sampling density was $Y_S = 1/1000$ mm.

Test	0.05 mm	0.10 mm	Means Comparison	Variance Comparison
Resolvability (N=10)	2.41 ± 0.020	2.43 ± 0.024	0.031	$p = 0.595$
Edge Width (N=10)	2.88 ± 0.036	2.80 ± 0.020	≈ 0	$p = 0.106$

Table 2. Effect of inter-line separation and sub-sampling density Y_S on the resolvability and edge width of an SG-102 laser line scanner. Each column shows the significance level of the ANOVA test, and groups within each row are significantly different if the significance level is less than 0.05. Significance levels less than 0.001 are represented as ≈ 0 and those larger than 0.999 are represented as ≈ 1 .

Test	Inter-line Separation	Y_S	Interaction
Resolvability (N=10)	≈ 0	0.023	0.931
Edge Width (N=10)	≈ 0	0.674	0.556

Inter-line Separation	0.05 mm	0.01 mm
Resolvability (N=40)	2.40 ± 0.018	2.42 ± 0.023
Edge Width (N=40)	2.87 ± 0.048	2.80 ± 0.024

Y_S	$1/2000$ mm	$1/1000$ mm	$1/500$ mm	$1/200$ mm
Resolvability (N=20)	2.41 ± 0.030	2.42 ± 0.025	2.42 ± 0.015	2.40 ± 0.012

with Table 1, N refers to the number of samples in each group, groups within each row are significantly different if the significance level is less than 0.05, a Tukey multiple-comparisons test was performed to determine which groups within each test are significantly different from each other at a significance level of less 0.050.

As can be seen in Table 2, inter-line separation once again had a significant effect on resolvability and edge width of the SG-102 laser line scanner. In both cases the inter-group difference is less than the 0.010 millimeter limit imposed by the Faro Gage Plus lateral measurement uncertainty so the results also have practical significance. Resolvability had a significant sub-sampling density effect, but the absence of an interaction effect indicates that the sub-sampling density main effect was consistent between inter-line separations. Multiple comparison testing determined that only the $1/500$ mm and $1/200$ mm groups were significantly different, but the inter-group separation in all cases was less than the Faro Gage Plus measurement uncertainty limit of 0.01 millimeters so this effect has no practical significance. In general, the resolvability and edge width metrics were relatively unaffected by sub-sampling density, with the resolvability structural resolution metric only being affected, albeit minimally, when the bin-to-bin separation is too large.

5. DISCUSSION

The step-response of a system indicates how it responds to sudden changes in surface distance that result in the laser spot being split over two surfaces with widely-varying distance from the 3D range scanner. Factors such as line width, the distance the spot moves during measurement, length of the triangulation system's baseline, and orientation of the step-edge with respect to the baseline axis all affect the size of the region affected by the step-edge. The slanted-edge test used in this study will always cross the baseline axis so some occlusion will always occur. The step-response of the 3D imaging system can be used to predict the 3dB response of the system to a pit; the width of the pit must be large enough that the magnitude of the response curve exceeds 0.707. Similarly, the step-response also can be used to predict the response of the system to a post-edge; the width of the post must be large enough that the magnitude of the response curve exceeds 0.707.

The inverse of the mean resolvability and edge width metric values represents the width of the affected and can also be reported as structural resolution values. The inverse resolvability varied from 0.41 to 0.42 mm and the inverse edge width varied from 0.35 to 0.36 mm, both figures being considerably larger than the quoted lateral resolution along either the x-axis (0.07 to 0.14 mm) or y-axis (≥ 0.02 mm). The discrepancy between quoted and measured resolution quantity values highlights the importance of establishing a consistent and commonly-accepted standard for quantifying the structural resolution of a 3D imaging system. In this study, repeated measurements and statistical analysis were used to ensure that any comparison of structural resolution values included the uncertainty inherent in the measurement process. Establishing

statistical validity is particularly important when comparing products to each other or to quoted values. Claims of product differences, or lack thereof, can have financial or legal repercussions so the approach presented in this paper includes an approach for within-product and between-product comparisons.

Experiments with varying the orientation of the step-edge with respect to the primary axis indicate that the edge width structural resolution metric can only be generated for systems with parallax if the sensor is located on the more distant side of the edge. This arrangement ensures that the sensor is never occluded, only the laser source, and results in an edge profile with sufficient curvature to locate the 3-dB drop point of both near and far surfaces.

The roof-response of a system indicates how it responds to sudden surface normal changes that result in the laser spot being partially or completely elongated, depending on the orientation of the roof-edge with respect to the baseline axis. Factors such as spot size, the distance the spot moves during measurement, length of the baseline, orientation of the edge with respect to the baseline axis, and orientation of the surface normal of both surfaces all affect the size of the region affected by the roof-edge. If the orientation of the normals of the roof surfaces is low enough then neither surface is occluded, making it relatively simple to obtain the spatial response curve. In this study the surface normals were approximately 45 degrees so occlusion was avoided; however, the angled surfaces would result in elongation of the laser spot which, in turn, results in an increase in measurement uncertainty.

6. CONCLUSIONS AND FUTURE WORK

Two test protocols have been developed and demonstrated for 3D imaging systems with significant parallax. The roof-response of the system is used to generate the resolvability structural resolution metric and the step-response of the system is used to generate the edge width structural resolution of the system. Only the edge-width metric were able to marginally detect the effect of changing inter-line separation of an SG-102 laser line scanner mounted on a translation stage on the structural resolution of the system. In general, if being able to resolve smaller features is considered better then systems with larger resolvability and edge width values are preferred over systems with smaller resolvability and edge width structural resolution values. Neither structural resolution metric on its own is sufficient to completely describe the structural resolution of a 3D imaging system, but the combination of edge width and resolvability structural resolution can be used to characterize two aspects of the structural resolution of the system. In all cases, the structural resolution values generated were larger than those reported in the SG-102 product specifications. Additional testing is required to examine the reproducibility of the resolvability and edge width metric values under a variety of conditions.

Future work will examine the effect of the relative difference in surface normals in peak surfaces on the ability to determine the roof-edge spatial frequency response. The surface normal orientations affect the measurement uncertainty that may increase the uncertainty of the roof-edge spatial frequency response values obtained from repeated measures testing; however, a smaller change in surface normal may make it more difficult to detect a change in the gain of the spatial response curve. Future work will also compare the step-response and pit-response of the system to determine if the step-response sufficiently predicts the pit-response that the pit-response does not need to be determined.

REFERENCES

1. JCGM 200:2008, *International Vocabulary of Metrology: Basic and General Concepts and Associated Terms (VIM)*. Working Group 2 of the Joint Committee for Guides in Metrology (JCGM/WG 2), BIPM, Pavillon de Breteuil F-92312 Sèvres Cedex, FRANCE, 3rd edition ed., 2008.
2. ASTM E 2544-08, *Standard Terminology for Three-Dimensional (3D) Imaging Systems*. American Society for Testing and Materials (ASTM International), West Conshohocken, PA, USA, April 2008.
3. ISO/IEC Guide 98-3:1995, *Uncertainty of measurement - Part 3: Guide to the expression of uncertainty in measurement (GUM)*. International Organization for Standardization (ISO), Geneva, Switzerland, 1995.
4. D. D. Lichti and S. Jamtsho, "Angular resolution of terrestrial laser scanners," *The Photogrammetric Record* **21**, pp. 141–160, June 2006.
5. J.-A. Beraldin, F. Blais, L. Cournoyer, M. Rioux, F. Bernier, and N. Harrison, "Portable digital 3-D imaging system for remote sites," in *Proceedings of the IEEE International Symposium on Circuits and Systems*, **5**, pp. 488–493, IEEE, 31 May–3 June 1998.

6. J.-A. Beraldin and M. Gaiani, "Evaluating the Performance of Close Range 3D Active Vision Systems for Industrial Design Applications," in *Proceedings of the SPIE: Videometrics IX*, **5665**, SPIE, (San Jose, CA, USA), 16-20 January 2005.
7. VDI/VDE 2617 Part 6.2, *Accuracy of coordinate measuring machines: Characteristics and their testing - Guideline for the application of DIN EN ISO 10360 to coordinate measuring machines with optical distance sensors*. The Association of German Engineers (VDI), 10772 Berlin, Germany, October 2005.
8. E. Trucco and A. Verri, *Introductory Techniques for 3D Computer Vision*, Prentice-Hall, Inc., Upper Saddle, NJ, 1998.
9. ISO 2854:1976, *Statistical interpretation of data - Techniques of estimation and tests relating to means and variances*. International Organization for Standardization (ISO), Geneva, Switzerland, 1976.
10. W. Mendenhall, *Mathematical Statistics with Applications*, PWS Publishers, Boston, Massachusetts, 3rd ed., 1986.
11. M. Goesele, C. Fuchs, and H.-P. Seidel, "Accuracy of 3D Range Scanners by Measurement of the Slanted Edge Modulation Transfer Function," in *Proceedings of the Fourth International Conference on 3-D Digital Imaging and Modeling*, IEEE, 2003.
12. ISO 12233:2000, *Photography - Electronic still-picture cameras - Resolution measurements*. International Organization for Standardization (ISO), Geneva, Switzerland, 2000.
13. ShapeGrabber, "SG2 Series Scan Heads - Metric Specifications." <http://www.shapegrabber.com/sol-products-3d-scan-heads-specs-metric.shtml>, 1 November 2003.
14. Faro Technologies, Coventry, UK, *Faro Gage and Gage-PLUS product specifications*, 12 December 2007.